A THREE-DIMENSIONAL STATIC NUMERICAL MODEL OF A COMPLEX UNDER-GROUND STRUCTURE IN HIGH SQUEEZING GROUND

Tina Marolt Čebašek *(corresponding author)*
University of Ljubljana,
Faculty of Natural Sciences and Engineering
Aškerčeva 12, 1000 Ljubljana, Slovenia
E-mail: tina.marolt@ogr.ntf.uni-lj.si

Jakob Likar
University of Ljubljana,
Faculty of Natural Sciences and Engineering
Aškerčeva 12, 1000 Ljubljana, Slovenia
E-mail: jakob.likar@ogr.ntf.uni-lj.si

Keywords
high squeezing ground, numerical model, underground structures, deformations, yielding support element

Abstract

The present study assesses high squeezing ground confirmed by empirical and semi-empirical theories. High squeezing ground is often present in underground constructions at great depths, but it is hardly ever researched separately from light and fair squeezing ground. A three-dimensional, static numerical model is developed for a complex underground structure consisting of a shaft, a silo, and a mine roadway at great depth, which is certainly in high squeezing ground. Furthermore, a solution for the entire structure based on shotcrete with incorporated yielding elements is provided. The yielding elements, in general, absorb the strain energy by compressing at a relatively constant stress, but without rebounding. A three-dimensional, static numerical model of a support system with incorporated yielding elements is established in order to demonstrate that the presented forces are under control. Therefore, a failure of the lining is avoided because the stresses in the shotcrete lining are below its load-bearing capacity. It can be concluded that yielding elements incorporated in the shotcrete lining play an important role in the support solution in high squeezing ground.

1 INTRODUCTION

The common view is that the excavation of underground structures through squeezing ground conditions is a very slow and hazardous process because the rock mass around the opening loses its inherent strength under the influence of the *in-situ* stresses [1]. Deformation can terminate during the construction or continue over a long period of time [2]. This study focuses on high squeezing ground conditions, confirmed by the theories of many authors [3,4,5,6,7,8]. The prediction of squeezing has also been made using experimental and critical stress methods [4]. Nowadays, research tends to focus on fairly and severe squeezing ground, but the main purpose of this paper is to explain and find a complete support solution for high and very heavy squeezing grounds. The challenge of this paper is the construction of shaft, silo, and a mine roadway through a rock mass with a low rock-mass quality value Q and a low uniaxial compressive strength σ_{cmass} . Various design options have been proposed and applied in Alpine tunnels [9]. The recent innovative technological developments in a yielding support system were implemented and proven in tunneling projects [10]. In this paper a three-dimensional, static numerical model of the structure in high squeezing grounds is created and the present study offers possible yielding support measures for high squeezing ground.

2 A REVIEW OF THE INDICATIONS OF HIGH SQUEEZING GROUND CONDITIONS

The high squeezing ground conditions are determined by two empirical approaches and four semi-empirical approaches in order to be certain that the structure is located in high squeezing ground.

Potential tunnel squeezing problems have been discussed by several authors and their definitions used in this study are listed below. In Singh's approach, based on an evaluation of squeezing and non-squeezing conditions, as in this case, the squeezing degree is not defined, but is based on the rock-mass quality Q and the overburden height H [8]. For the squeezing conditions the value should satisfy the equation $H>>350\ Q^{1/3}$. Furthermore, it is established that the tangential stress failure may be double the *in-situ* stress p_0. In other words, the rock-mass uniaxial compressive strength σ_{cmass} can be calculated as follows [11]:

$$\sigma_{cmass} = 0.7\gamma Q^{1/3} \text{ [MPa] for } Q<10. \qquad (1)$$

where γ is the rock-mass unit weight (MN/m^3) and Q is the rock-mass quality.

This equation is also logically justified when the rock mass quality Q is obtained soon after excavation in nearly dry, weak rock masses. This equation also explains why the squeezing criterion is found to be independent of the uniaxial compressive strength and so its correction is not needed [1,4,10].

Goel explained a theory that is based on the rock-mass number and considers the overburden height H and the tunnel diameter B [5]. The degree of squeezing is defined as high squeezing at 5% of the normalized tunnel squeezing ε_t. See Table 1.

Jethwa included the data on the degree of squeezing in relation to the ratio of the rock-mass uniaxial compressive strength σ_{cm} and the *in-situ* stress p_0. The solution of the type behaviour is described as highly squeezing only when the degree of squeezing is less than 0.4 [7]. See Table 1.

Aydan's criterion assumed that the rock-mass uniaxial compressive strength σ_{cmass} and the uniaxial compressive strength of the intact rock are the same σ_c [3]. The squeezing level is described as heavy squeezing when the ratio of the peak tangential strain ε_p at the periphery of the tunnel and the elastic strain limit ε_e, also known as the elastic state ς, is greater than the ratio of the critical strain limit ε_s and the elastic strain limit ε_e, but lower than the ratio of the residual strain limit ε_r and the elastic strain limit ε_e (see Table 1). The strain limits are explained in Figure 1. In order to simplify the comparison of the different theories, it is considered that a heavy squeezing condition corresponds to a high squeezing condition.

Barton's criterion is similar to Ayden's, and the squeezing level is described by the squeezing index *SI*. The very heavy squeezing condition corresponds to values greater than 5 and the heavy squeezing condition corresponds to values between 3 and 5 [4] (see Table 1). According to the uniaxial compressive strength, the intact rock is assumed to be 1 MPa. The *SI* corresponds to the ratio between the observed, or the expected, strain and the critical strain. Several levels of squeezing based on the ratio between the expected strain and the critical strain:

$$SI = \frac{\frac{u}{r_0}}{\varepsilon_{cr}} \qquad (2)$$

where u is the radial closure, ε_{cr} is the critical strain and r_0 is the radius of the opening.

The values of the critical strains are obtained from the numerical modelling in this study, but they could also be obtained from actual monitoring. In order to simplify the comparison of different theories, it is considered that a heavy squeezing condition corresponds to a high squeezing condition.

Finally, Hoek's approach is used for the evaluation of squeezing problems. It is considered that very severe squeezing problems occur when the tunnel strain ε_t is between 5% and 10%, and extreme squeezing problems occur when the tunnel strain ε_t is larger than 10% [7]. In order to simplify the comparison of the different theories, it is considered that very severe squeezing problems correspond to a high squeezing condition.

The presented approaches are limited to a high and a very heavy squeezing condition, and they are presented Table 1.

2.1 Squeezing classification

The potential squeezing problems of the mine roadway are evaluated using Equation 3, and the ultimate support pressure in the squeezing ground condition is evaluated according to Equation 3, where in this study a rock-mass

Table 1. Review of approaches.

	Empirical approach		Semi-empirical approach			
	Singh	Goel	Jethwa	Aydan	Barton	Hoek
HS	-	$\varepsilon_t > 5\%$ of B	$\sigma_{cm}/p_0 < 0.4$	$\varepsilon_s/\varepsilon_e < \varsigma < \varepsilon_r/\varepsilon_e$	$3 < SI \leq 5$	$5\% < \varepsilon_t < 10\%$
VHS	-	-	-	$\varepsilon_r/\varepsilon_e < \varsigma$	$5 < SI$	$10\% < \varepsilon_t$
S	$H >> 350\ Q^{1/3}$	$\varepsilon_t > 1\%$ of B	$\sigma_{cm}/p_0 < 2$	$1 < \varsigma$	$1 < SI$	$1\% < \varepsilon_t$

HS – high squeezing, VHS – very heavy squeezing, S – squeezing

quality Q with SRF=1 and the correction factor f for the tunnel closure obtained for a high degree of squeezing is used [12,13,14].

$$\varepsilon_t = 0.15\left(1-\frac{p_i}{p_0}\right)\frac{\sigma_{cm}^{-\left(\frac{3p_i}{p_0}+1\right)/\left(\frac{3.8p_i}{p_0}+0.54\right)}}{p_0} \qquad (3)$$

where ε_t is the tunnel strain, p_i is the support pressure, σ_{cm} is the rock-mass uniaxial compressive strength, and p_0 is the *in-situ* stress.

$$p_{sq} = \left(\left[\frac{f}{30}\right]\cdot 10^{-\left[\frac{H^{0.6}\cdot\left(\frac{B}{2}\right)^{0.1}}{50\cdot N^{0.33}}\right]}\right) r \qquad (4)$$

where p_{sq} is the estimated ultimate support pressure in the squeezing ground conditions, f is the correction factor for the tunnel closure, N is the rock-mass number, H is the overburden height, B is the diameter of the tunnel, and r is the correlation coefficient.

It is important to precisely evaluate the degree of squeezing because underground construction in the squeezing ground is very demanding due to the difficulty in making a reliable prediction in the design stage. For the study of the squeezing potential a program in MATLAB is written, where the squeezing classification is based on empirical equations and inequalities from Table 1 and other model characteristics obtained from the numerical modeling and laboratory tests. The final results are presented in Table 2.

2.3 Laboratory testing and rock description

The properties of the model material are defined by a laboratory test that was carried out by testing specimens in order to analyse the strength and the strain behaviour under a uniaxial stress state, where ε_p is the peak strain limit, ε_s is the critical strain limit, ε_e is the elastic strain limit, ε_r is the residual strength limit, σ_p is the peak stress, and σ_r is the residual stress (Figure 1). Generally, very weak to weak sedimentary rocks with a typical uniaxial strength between 1 MPa and 3 MPa are presented at the investigated depths (Figure 2). The uniaxial compression tests were carried out using an electronically controlled hydraulic press with a capacity of 1150 kN. The velocity during the test was 1 mm/min. The vertical displacements and the normal force were measured and the numerical modeling is conducted with the same force-strain behavior as shown in Figure 1. For modelling a three-dimensional, static numerical model the results of one specimen are used for reasons of simplicity.

Table 2. Analysis of the selected data.

Structure	Overburden height (m)	*In-situ* stress (MPa)	Empirical approach		Semi-empirical approach			
			Singh	Goel	Jethwa	Aydan	Barton	Hoek
Shaft	448	9.86	*S*	*VHS*	*HS*	*VHS*	*VHS*	HS_p
Mine roadway	468	10.30	*S*	*VHS*	*HS*	*HS*	*VHS*	HS_p
Silo	484.5	10.66	*S*	*VHS*	*HS*	*HS*	*VHS*	HS_p
Shaft	500	11	*S*	*VHS*	*HS*	*HS*	*VHS*	HS_p

HS – high squeezing, VHS – very heavy squeezing, S – squeezing, index *p* refers to problems.

Due to the geological conditions given in Figure 1, the squeezing level is obtained from critical strains. The typical uniaxial compressive strength is 1.25 MPa, the rock-mass quality Q is 0.16, and the unit weight is 22 kN/m^3.

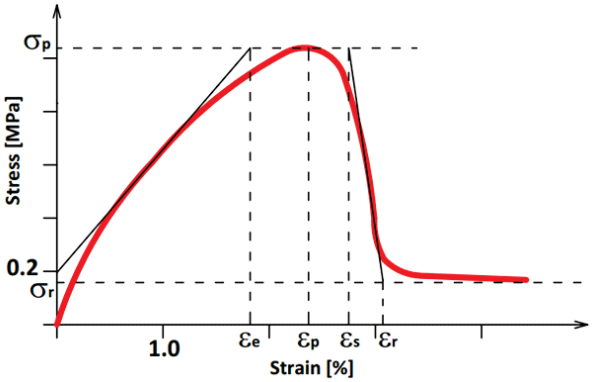

Figure 1. Strain limits of the subjected high squeezing ground.

For each sample from Figure 2 the squeezing index is provided. It is clear from Figure 3 that the upper part of the shaft is under very heavy squeezing conditions and the other parts of the underground structures are under high squeezing conditions. This is also summarized in Table 2.

It is obvious from Figure 3 that the squeezing level of the investigated samples is relatively high, and for that reason it can be concluded that the three-dimensional, static numerical model is set in high to very heavy squeezing ground. These results suggest the need for further research and modelling.

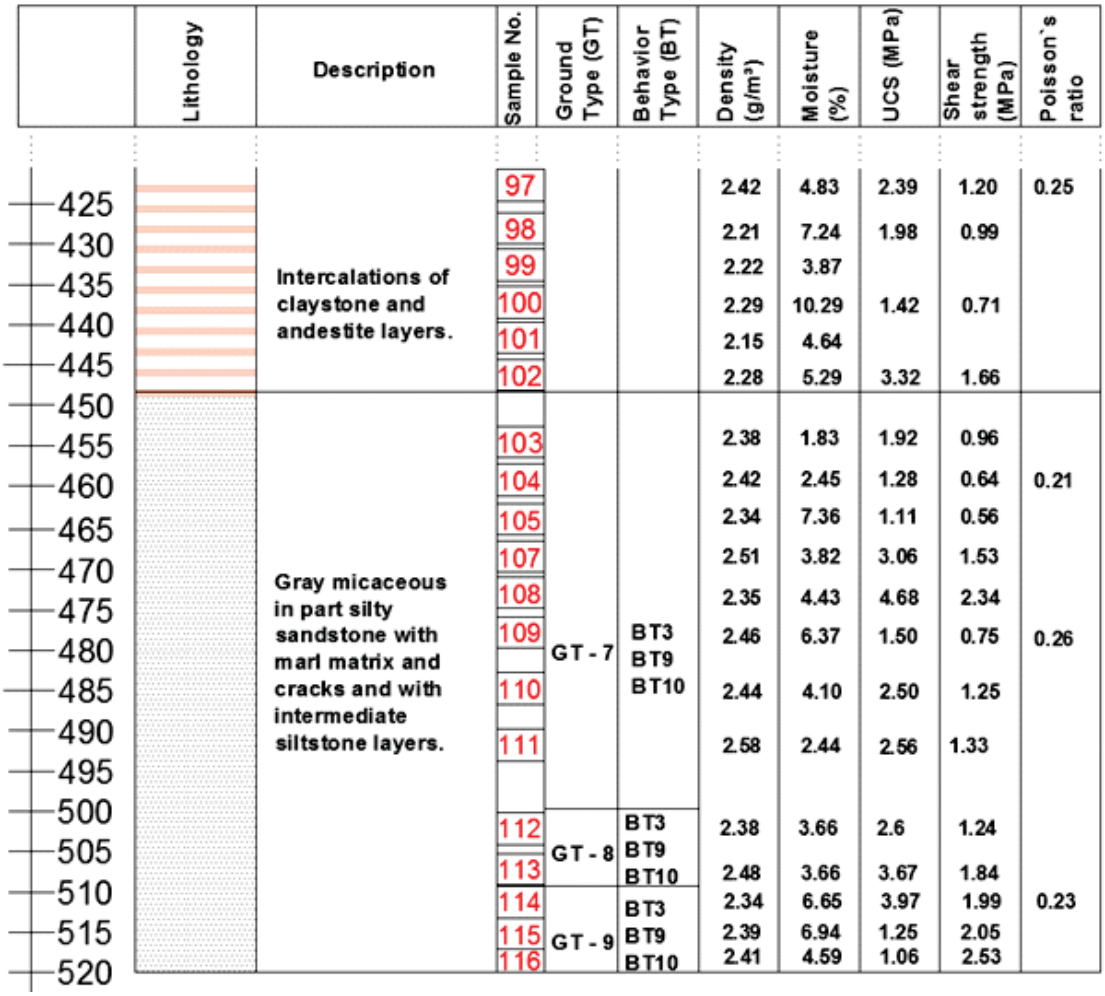

Figure 2. Geological conditions.

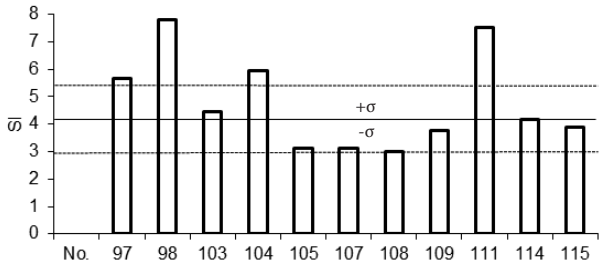

Figure 3. The squeezing level of the investigated samples.

3 A THREE-DIMENSIONAL, STATIC NUMERICAL MODEL

3.1 The Model

The analyses are carried out in order to identify the critical strains and stresses using the Midas GTS (Geotechnical and Tunnel Analysis system) software, which also enables modelling of unconventional interconnections in underground structures [15]. This is the main reason why it is used in this issue. Finite-element software and a three-dimensional, static numerical model of the study are established. The numerical analyses are performed on an idealised shaft, a silo, and a mine roadway in the idealized high squeezing grounds. The complex underground structure is excavated to a depth between 427.3 m and 519 m. In all the analyses and calculations the time development of the ground pressure of the high squeezing ground is not taken into account. It is included as a final maximum ground pressure, which is applied on the primary shotcrete lining of the shaft.

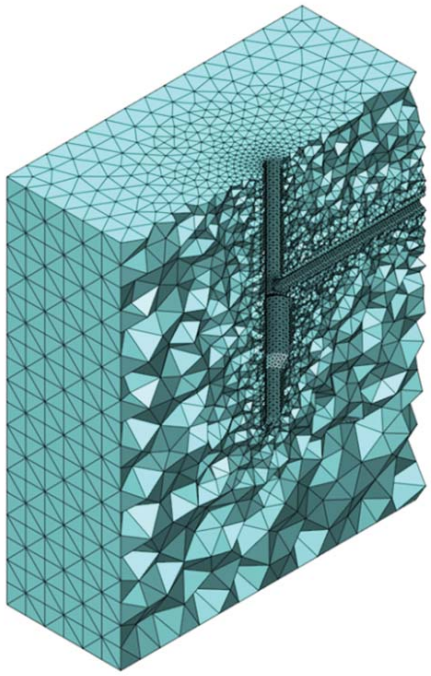

Figure 4. The mesh of a 3D computation model that is divided into 406,990 elements and 68,658 nodes.

The total size of the model is 120 m × 100 m × 150 m (Figure 4) and the input parameters are presented in Table 3. The high squeezing ground is simulated by specific, four-noded, tetrahedron elements with Mohr-Coulomb's ideal elastic-plastic constitutive material model. Furthermore, a von Mises yield criterion is used for the yielding elements, and shotcrete is simulated by plane triangular elements with Mohr-Coulomb's ideal elastic-plastic constitutive material model. Ultimately, all the elements are connected into the discretization points. The horizontal movement is limited on the sides; the vertical and horizontal movements are limited on the bottom; and the top of the model is a free surface. The length of the mine roadway is 60 m and the diameter is 4.6 m. It is positioned 466.9 m below the surface; the shaft's diameter is 6.4 m; the silo is placed at a depth between 474 m and 495 m, and its diameter is 10 m.

The process is simulated in 36 stages; the shaft dipping (sinking) and the mine roadway excavation begin at the same time. The mine roadway's excavation is conducted from the edge in the direction of the silo. During the first stage, the primary stress state condition is analysed; during the second-stage excavation a 3-m-long excavation step is simulated; and in the third stage the next excavation step follows and is of the same length as in the previous step. Meanwhile, the primary lining in the second stage is being applied and the characteristics of the primary lining are used for applying young shotcrete. Simultaneously, the yielding elements are being installed in a three-dimensional, static numerical model with incorporated yielding elements. During the fourth stage the third excavation step is simulated and the installation of the primary lining with young shotcrete characteristics is described as well. At the same time, the yielding elements are being installed in a three-dimensional, static numerical model with incorporated yielding elements. At that point in the second phase, the characteristics of the hardening shotcrete are considered. The process of excavating and supporting is repeated until stage 36. The explanation of this process is presented in Figure 5, and the characteristics of model, in Table 3. A numerical simulation without yielding elements is carried out in the same sequences, but the yielding elements are omitted.

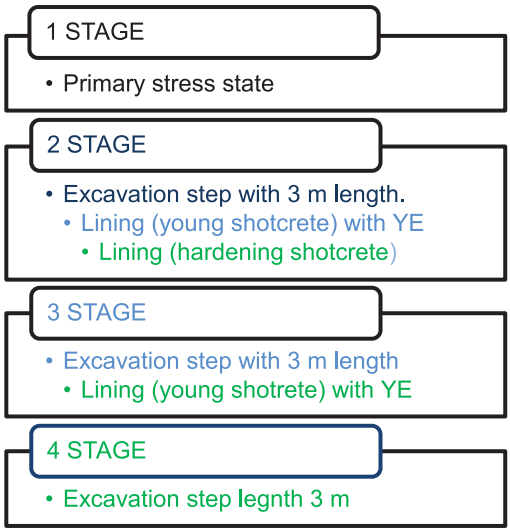

Figure 5. Explanation of stages to the point when the process starts repeating until the 36th stage.

The shaft sinking was stopped at stage 16, and this is 474 m below the surface. The mine roadway's excavation continued in three isolated stages. The shaft and the mine roadway were connected at stage 19. Finally, the silo and the last part of shaft sinking were implemented.

3.2 Displacements

The displacements of the nodes in the model without the yielding elements' integration are analysed in Figure 6. The nodes are placed on the shotcrete lining and their displacements vs. stages are investigated in the shaft at stage 7, which is 448 m below the surface; in the mine roadway at stage 10, which is 468 m below the surface; and in the silo at stage 24, which is 484.5 m below the surface. The approximate location of the nodes for a better visualisation can be seen in Figure 9, and these nodes are investigated in the model without the yielding elements' integration.

Table 3. Details of the reference case.

	Squeezing ground	Young shotcrete	Hardening shotcrete	Yielding element
Modulus of elasticity (MPa)	700	3 000	20 000	150
Unit Weight (MN/m^3)	0.022	0.025	0.025	0.0785
Poisson's ratio	0.3	0.2	0.2	0.3
Model Type	Mohr-Coulomb's ideal elastic-plastic			Von Mises
Uniaxial compressive strength (MPa)	1.25	10	32	-
Yield stress (MPa)	-	-	-	4.5
Thickness (m)	-	0.25	0.25	0.25

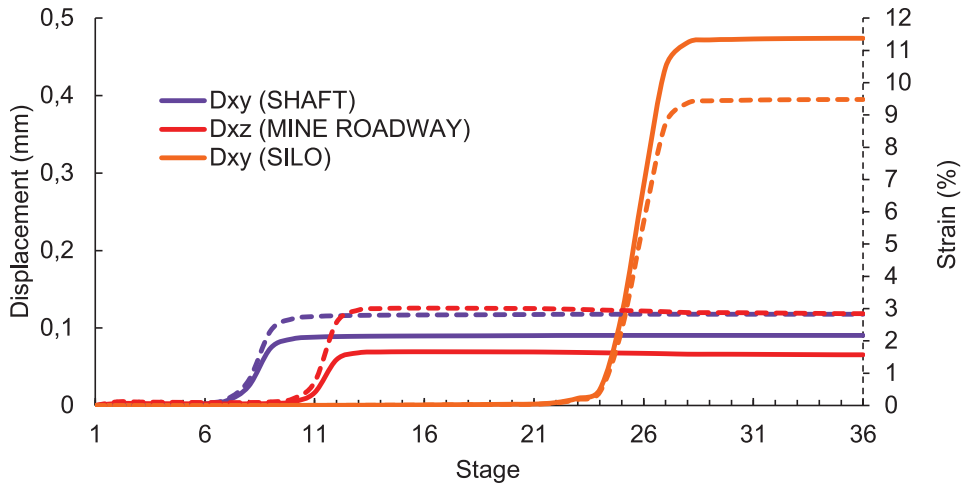

Figure 6. The tunnel shotcrete lining deformation against the stages and values indicate the movement towards the centre of the mine roadway, the shaft, and the silo.

It is considered that the shotcrete lining can withstand 1% of strain deformation; higher deformations lead to a collapse [10,16]. It is clear from Figure 6 that the maximum strain deformation of the shotcrete is exceeded and amounts to 2.85% in the mine roadway, 2.92% in the shaft, and 9.48% in the silo. This means that the shotcrete is an inappropriate support solution when dealing with high squeezing ground.

In addition, the stability of the shaft, the silo, the mine roadway, and the wall rock are investigated with a numerical method; this is a three-dimensional structure and requires three-dimensional modelling for a proper understanding. The displacements actually occur at the periphery of the openings and may be obtained for the shaft, as well as for the silo with displacements in the XY direction (Figure 7, Figure 8) and for the mine roadway with displacements in the XZ direction (Figure 7).

It should be noted that the critical strain is an anisotropic property and it is different in different points at the periphery of the openings. The expected critical strain at the periphery of the openings depends on the size and the shape of the openings, as well as on the *in-situ* stress state, and on the rock-mass properties. A simulation is made in 3D conditions, and displacements of 116 mm in the wall rock of the shaft and the mine roadway are usually expected (Figure 7). These displacements are incomparably lower than the displacements in the wall rock of the silo. For this reason, Figure 8 shows the displacements towards the end of the simulation. It is clear that displacements of 539 mm occur at this point.

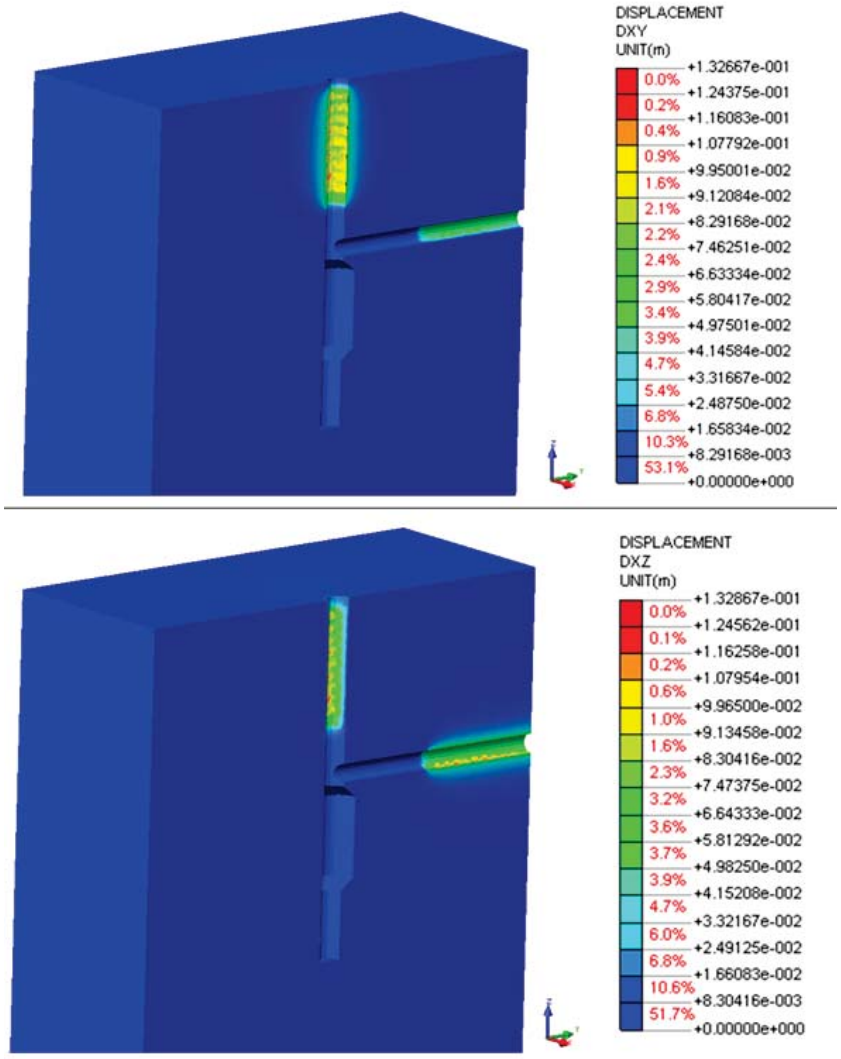

Figure 7. The displacement investigation at the periphery of the openings at stage 10 for the shaft and mine roadway, respectively.

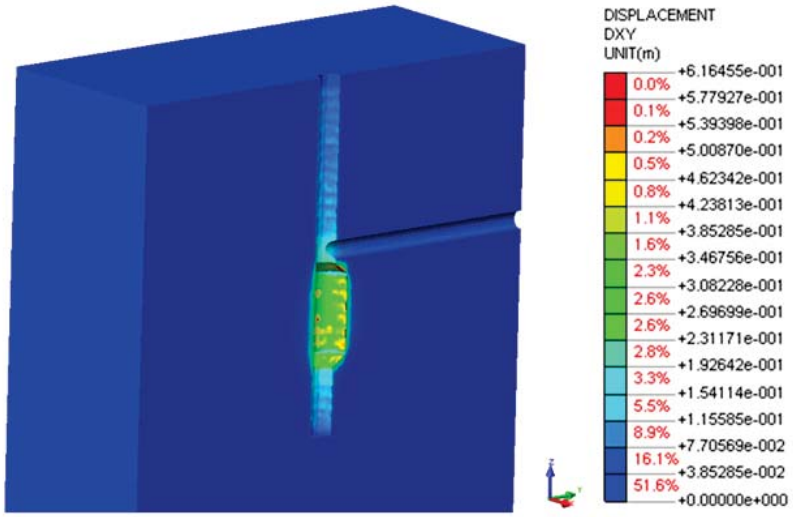

Figure 8. The displacement investigation at the periphery of the shaft and silo at stage 34.

The obtained evidence proved that there is no doubt we are dealing with a high squeezing ground condition.

Therefore, the three-dimensional, static numerical model could be completed for a prediction of the squeezing problem's evaluation. The obtained results show that the underground structure is positioned in high squeezing ground. For this reason, appropriate support measures must be ensured.

4 A SOLUTION FOR THE SUPPORTING PROBLEMS IN HIGH SQUEEZING GROUND

4.1 Yielding elements

In this study the shotcrete lining is accommodated with yielding elements because the shotcrete lining is one of the most commonly used support elements. The thickness of the shotcrete lining is 250 mm. In addition, the shotcrete shell is improved by using yielding elements that are incorporated into the shotcrete lining (Figure 9), thus allowing a controlled transfer of the stress across the longitudinal gaps. Their construction is relatively simple, and the structure consisted of four sets provided by Midas GTS.

The numerical modeling is undertaken to predict the deformability in the desired manner. The suitable yielding element in these circumstances is designed for a

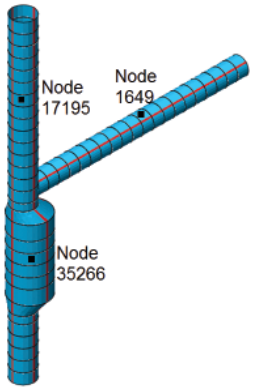

Figure 9. Model with yielding support system and incorporated yielding elements (red color) and shotcrete (blue color).

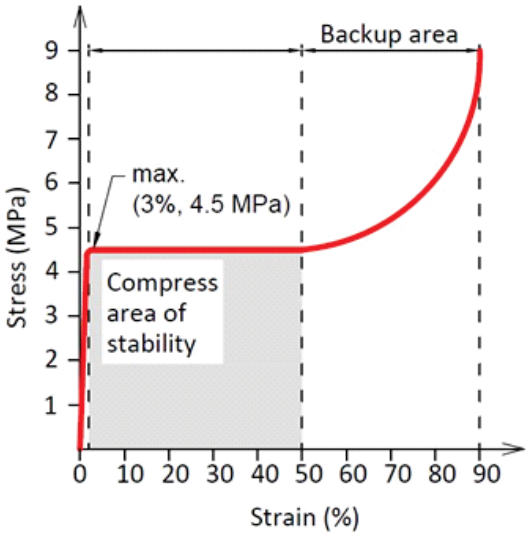

Figure 10. Stress vs. strain of yielding element.

load level of 4.5 MPa, which is reached at a strain of 3% (Figure 10). The compressed area of stability is from 3% to 59% strain, which represents the ideal energy absorption. Above a 59% strain the backup zone is reached, which represents the energy-absorption reserve, although the shotcrete line is expected to take over the entire load. The tests concerning the ductile behavior of the yielding elements made clear the required deformability for the purposes of the construction.

4.2 Stresses and forces

The maximum and minimum tangential stresses appear in the Y direction for the shaft and in the X direction for the mine roadway. This is significant because the maximum and minimum radial stresses appear in the Y direction for the shaft and in the Z direction for the mine roadway in the global coordinate system. The gravitational stress, which is essential for the shaft and the silo, is considered along the Z direction. A detailed analysis is made for the nodes on the shotcrete lining in the model with the incorporated yielding elements, an approximated position of the nodes is presented in Figure 9, and the results of the analysis are presented in Figure 11. The yielding elements used in this analysis are suitable. The tangential forces increased in the yielding elements and the compressive strength is not exceeded at any stage of the construction. This is logical and the main goal of controlled deformation is achieved.

Figure 11 shows the calculated values of the normal stresses S_{XX}, S_{YY}, and S_{ZZ} depending on the simulated stage of the construction of the analyzed mine roadway, shaft, and silo. The main difference between the calculated stresses in the early simulation stages of excavation – shaft sinking and installation of primary support system – is seen in the stress magnitudes at the periphery of the silo, with half value stresses at the periphery of the mine roadway, and at the upper part of the shaft that is analyzed. The main reason for this stress redistribution is in the chronological simulation of the construction of these underground facilities, which in practice represents a complex system of underground structures for the purposes of the shaft's operation. In addition, the element coordinate system for a detailed analysis is used. Generally, the force distribution of the shaft and the silo lining in the X direction (Figure 12) of the local coordinate system is taken into consideration. The maximum part of the shaft area is under 2.9 MN/m, and the maximum part of the silo area is under 6.8 MN/m. The critical area of the forces is located in the infinitesimal part of the silo and it is proposed that it could be stabilized by a thicker shotcrete lining or by a shotcrete with a higher compressive strength class. If the critical forces would be spread over the larger part of the structure it could be stabilized with the numerous deformable elements in the lining. This is a reasonable option with respect to a symmetric distribution of them, where the large strains are expected. It can be concluded that the size of the forces depends on the dimensions of the underground structures [10].

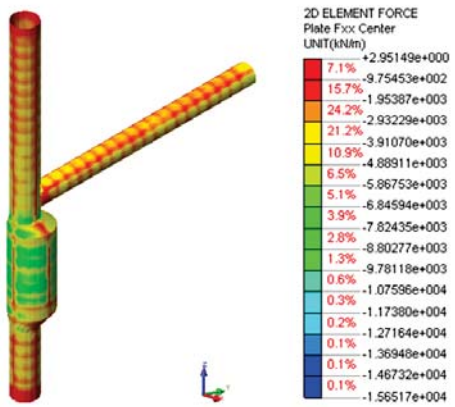

Figure 12. Tangential forces of underground structures in the element coordinate system.

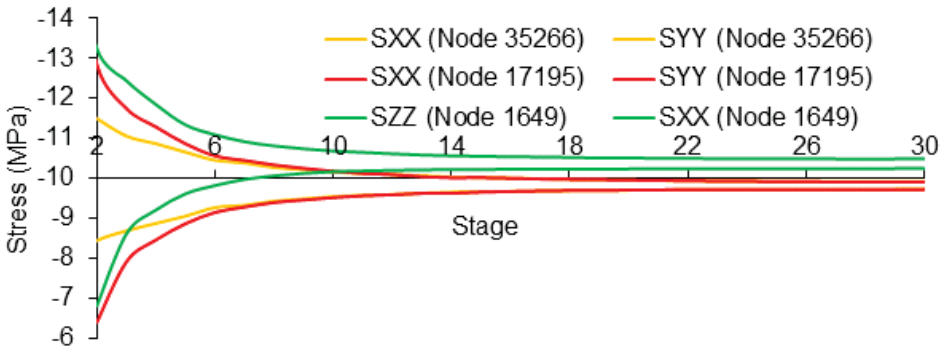

Figure 11. Tangential and radial stresses for mine roadway, shaft and silo.

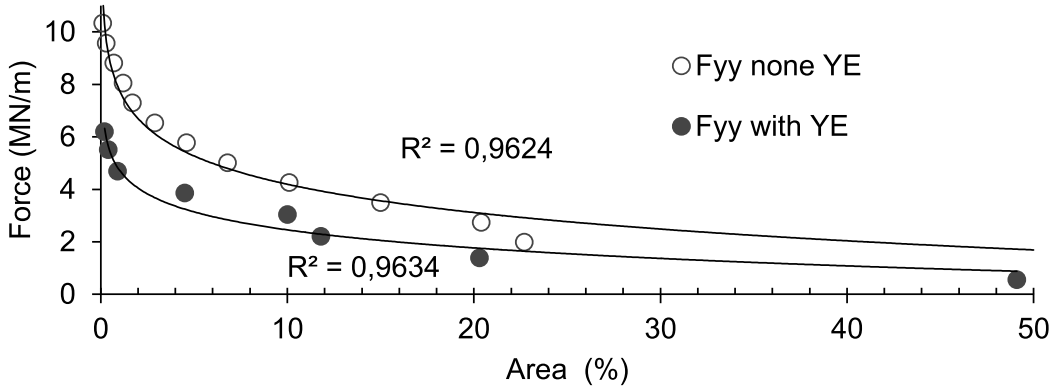

Figure 13. Tangential forces of the mine roadway with and without the incorporated yielding elements.

Moreover, a study with and without the incorporated yielding elements is made for the mine roadway, which is analysed in the Y direction in the local coordinate system. The force distributions are more favourable and generally are 40 % lower with the incorporated yielding elements. This means that almost half of the area is under the lowest force value and the compressive strength of the shotcrete is not exceeded at any force level if support measures with incorporated yielding elements (Figure 13) are applied.

5 DISCUSSION

Critical strain plays an important role in the determination of squeezing problems [17]. In this study the critical strain is obtained from numerical modelling, otherwise it could also be obtained from actual monitoring from the field, as in the Saint Martin La Porte access tunnel [10]. The magnitude of the tunnel's convergence, which is obtained by numerical modelling, ensures a prediction of the allowable space that is needed to accommodate the ground deformation. With this procedure the re-profiling is avoided in the construction stage as it was needed in Yacambú–Quibor Tunnel [13]. With numerical modeling, the additional costs could be avodied during the design stage. The full-face excavation method has been proved to be approprite in case studies of the Saint Martin La Porte access tunnel and the Lyon-Torino Base Tunnel [18]. There, also, the recently established yielding elements were used. For that reason the full excavation method is used in this study. This method provides a large working space and there large equipment can be effectively used for the installation of the appropriate support measures. The procedure of the evaluation of the degree of squeezing is described from laboratory tests and data obtained from numerical modelling. It is supposed that the squeezing level cannot be precisely predicted from samples, but it is obvious that the dimensions of the underground structure have a major influence on the developed displacements and the stress changes.

6 CONCLUSION

This study's main focus was on high squeezing ground behaviour, as it is not commonly investigated separately from other squeezing degrees, but often appears in underground excavations. The results of the explained analysis provide a solution for supporting a complex underground structure in high squeezing ground at great depths. The main aim of the present analysis is to find the proper yielding element, which has the proper rigidity, and helps reduce the stresses in the shotcrete lining. It could be concluded that the yielding elements incorporated into the shotcrete lining play an important role in the support measures in high squeezing ground to guarantee the stability of the support systems in all the stages of the construction, and the operation of the shaft.

Acknowledgements

The authors would like to express their sincere gratitude to Innovative Scheme for Co-Financing Doctoral Studies.

REFERENCES

[1] Aydan, O., Akagi, T., Kawamoto, T. 1996. The squeezing potential of rock around tunnels, theory

and prediction with examples taken from Japan. Rock mechanic and rock engineering 29, 125-143.
[2] Barla, G. 1995. Squeezing rocks in tunnels. ISRM News J 3(4), 44-49.
[3] Aydan, O., Akagi, T., & Kawanoto, T. 1993. The squeezing potential of rocks around tunnels. Rock Mechanics and Rock Engineering 26(2), 137-163.
[4] Barton, N. 2002. Some New Q Value Correlations to Assist in Site Characterisation and Tunnel Design. International Journal of Rock Mechanics and Mining Sciences 39, 185-216.
[5] Goel, R., Jethwa, J., Paithankar, G. 1995. Tunnelling through the young Himalayas — A Case History of Maneri–Uttarkashi Power Tunnel. Engineering Geology 39, 31-44.
[6] Jethwa, J., Singh, B. 1984. Estimation of Ultimate Rock Pressure for Tunnel Linings under Squeezing Rock Coditions—A New Approach. In Proccedings of ISRM Symposium on Design and Performance of Underground Excavations, pp. 231-238. Cambridge: Brown, E.T., Hudson, J.A.
[7] Hoek, E. 2001. Big Tunnels in Bad Rock. Journal of Geotechnical and Geoenvironmental Engineering 127, 726-740.
[8] Singh, B., Jethwa, J., Dube, A. 1992. Correlation between observed support pressure and Rock Mass Quality. Tunnelling and Underground Space Technology 7, 59-74.
[9] Schubert, W. 1996. Dealing with squeezing conditions in Alpine tunnels. Rock Mechanics and Rock Engineering 29(3), 145-153.
[10] Barla, G., Bonini, M., Semeraro, M. 2011. Analysis of the Behaviour of a Yield-Control Support System in Squeezing Rock. Tunnelling and Underground Space Technology 26, 146-154.
[11] Singh, B., & Goel, R. K. 1999. Rock Mass Classification. Elsevier.
[12] Goel, R., Jethwa, J., Dhar, B. 1996. Effect of Tunnel Size on Support Pressure. International Journal of Rock Mechanics and Mining Sciences 33(7), 749-755.
[13] Hoek , E., Guevara, R. 2009. Overcoming Squeezing in the Yacambú–Quibor Tunnel, Venezuela. Rock Mechanics and Rock Engineering 42, 389-418.
[14] Hoek, E., & Marinos, P. 2000. Predicting Tunnel Squeezing Problems in Weak Heterogeneous Rock Masses. Tunnels & Tunnelling International 45-51 (part 1), 33-36.
[15] MIDAS IT Co. Ltd. 2002. Basic & Advanced Tutorials. Beijing.
[16] Kovári, K. 2003. History of the Sprayed Concrete Lining Method – Part I. Tunnelling and Underground Space Technology 18, 57-69.
[17] Singh, M., Singh, B., Choudhari, J. 2007. Critical Strain and Squeezing of Rock Mass in Tunnels. Tunnelling and Underground Space Technology 22, 343-350.
[18] Barla, G. 2009. Innovative tunnelling construction method to cope with squeezing at Saint Martin La Porte access adit (Lyon-Torino Base tunnel). Dubrovnik, Croatia: Rock Engineering in Difficult Conditions in Soft Rocks and Karst. Proceedings of Eurock. ISRM Regional Symposium.